

Asymptotic Performance Analysis of Free-Space Optical Links with Transmit Diversity

Jianfeng Feng and Xiaohui Zhao*

College of Communication Engineering, Jilin University, Changchun 130012, P. R. China

(Received January 25, 2016 : revised May 2, 2016 : accepted June 14, 2016)

The misalignment errors and fluctuations in irradiance due to atmospheric turbulence can severely degrade the performance of free-space optical (FSO) systems. In this paper, we investigate the asymptotic bit error rate (BER) performance and diversity orders of FSO links using parallel transmit-diversity schemes. The BER expressions of FSO links with the switch-and-examine transmit (SET), switch-and-examine transmit with post-selection (SETps), dual-branch transmit laser selection (Dual-TLS), and group transmit laser selection (Group-TLS) schemes are derived, based on an approximate channel model. Then numerical simulations for these four schemes in the region of high average signal-to-noise ratio (SNR) are presented under different channel conditions. The results show that the four transmit-diversity schemes can reduce system complexity and overcome the limitation of peak power, without much BER deterioration.

Keywords : Free space optical communication, Performance analysis, Transmit diversity, Bit error rate
OCIS codes : (010.1290) Atmospheric optics; (010.1330) Atmospheric turbulence; (010.3310) Laser beam transmission; (060.4510) Optical communications

I. INTRODUCTION

FSO communications are potential solutions for a variety of applications, such as last-mile communications, fiber backup, and disaster-recovery communications [1]. Compared to traditional radio-frequency (RF) communications, their advantages include high speed, unlicensed spectrum, and excellent security [2]. However, FSO communications are vulnerable to pointing errors and scintillation. Both pointing errors from the misalignment between transmitters and receivers and the scintillation from atmospheric turbulence can seriously deteriorate communication quality [3].

To overcome these disadvantages, many technologies have been applied in FSO systems, such as adaptive optical (AO) systems, error correct coding (ECC), and relay-assisted transmission. BER performance and channel capacity of an FSO system with AO are studied in [4, 5]. Upper bounds on the pairwise code-word-error probability for coded FSO communication systems through atmospheric turbulence channels are obtained in [6, 7]. In [8], relay-assisted transmission is shown to be an effective tool to mitigate fading for FSO systems operating in atmospheric turbulence channels. A

one-relay cooperative diversity scheme is proposed and analyzed for noncoherent FSO communications with intensity modulation and direct detection (IM/DD) in [9]. A novel adaptive cooperative protocol with multiple relays over atmospheric turbulence channels with pointing errors is given in [10].

Spatial diversity is a powerful technique to mitigate the effects of fading in both traditional radio-frequency (RF) and FSO communications. However, unlike an RF signal with broadcast characteristics, the optical signal in an FSO system is usually transmitted from point to point through a line-of-sight path. Therefore, the concept of spatial diversity in FSO differs from that in traditional RF communications. As introduced in [11], spatial diversity in FSO systems can be realized via the use of multiple apertures at the receiver (receive diversity) [12], multiple beams at the transmitter (transmit diversity) [13-15], or a combination of the two [16-23]. Receive diversity and transmit diversity are usually referred to as SIMO (Single-Input Multiple-Outputs) and MISO (Multiple-Inputs Single-Output) respectively. Meanwhile, a system using both receive and transmit diversity is referred to as MIMO (Multiple-Inputs Multiple-Outputs).

For SIMO systems, effectiveness of the two receive-diversity

*Corresponding author: xhzhao@jlu.edu.cn

Color versions of one or more of the figures in this paper are available online.



This is an Open Access article distributed under the terms of the Creative Commons Attribution Non-Commercial License (<http://creativecommons.org/licenses/by-nc/3.0/>) which permits unrestricted non-commercial use, distribution, and reproduction in any medium, provided the original work is properly cited.

solutions, i.e. aperture averaging and multiple apertures, are compared in [12]. For MISO FSO systems, the simplest transmit-diversity scheme is to send the same signal on different beams, which is usually referred to as repetition coding (RC) [15]. Performance of two other typical transmit-diversity schemes, transmit laser selection (TLS) and multiuser diversity (MD), are presented respectively in [13, 14]. For MIMO FSO systems, approximated expressions of average bit-error probability (ABEP) are derived in [16-18]. The outage performance for MIMO FSO communication systems with on-off keying (OOK) and pulse-position modulation (PPM) are analyzed in [19, 20]. Performance analysis of Gamma-Gamma fading FSO MIMO links with pointing errors is presented in [21]. ABEP of uncoded and optical spatial modulated MIMO FSO systems is derived in [22]. In [23], ergodic capacity characterization of MIMO FSO systems over atmospheric turbulence-induced fading channels is studied. In particular, for SIMO and MIMO FSO systems, equal-gain combining (EGC) and maximal-ratio combining (MRC) are usually performed at the receiver. For MISO systems with RC, EGC is the default combining scheme.

In order to understand well the communication quality offered by different FSO systems for real applications, it is necessary to analyze the performance of the systems. BER is the most effective evaluation metric to demonstrate this quality. In this paper, we introduce four new parallel transmit-diversity schemes in FSO links, namely, switch-and-examine transmit (SET), switch-and-examine transmit with post-selection (SETps), dual-branch transmit laser selection (Dual-TLS), and finally group transmit laser selection (Group-TLS) for communication performance analysis. Particularly, SET and SETps switch to other diversity branches only when an outage occurs, hence they have a simpler structure and lower processing load than the traditional TLS scheme. Dual-TLS and Group-TLS are two multibranch TLS schemes that can meet the peak-power and eye-safety constraints.

In this paper, we derive asymptotic average BER expressions for the four transmit-diversity schemes above, based on an approximate channel model. Then we discuss system complexity, from the aspects of hardware structure, channel estimation rate, and lowest feedback transmission rate. Numerical simulations for the region of high average signal-to-noise ratio (SNR) are presented under different channel conditions.

To further illustrate the performance of the four transmit-diversity techniques, we also present the BER curves for FSO systems with traditional TLS or RC as benchmarks. Assuming the same total transmit power and total noise, the BER curve of a MISO FSO system using MRC diversity is also given for comparison. Based on simulation results, analysis of the asymptotic BER performance of the four parallel transmit-diversity schemes is provided.

The remainder of this paper is organized as follows. Section II describes the FSO system model and the approximate atmospheric optical channel model. In addition, we derive a statistical model of channel gain in a MISO FSO communication system. In Section III, we give asymptotic BER expressions for SET, SETps, Dual-TLS, and Group-TLS, based on the channel model described in Section II. In section IV, we conduct the complexity analysis for the four parallel diversity FSO systems. Section V presents some numerical results, and Section VI makes several important conclusions.

II. SYSTEM AND CHANNEL MODEL

2.1. System Model

A MISO FSO communication system is illustrated in Fig. 1. It consists of an OOK modulator, a switch control unit and N laser sources at the transmitter, and a photoelectric detector and channel estimator at the receiver. The spacing between the N laser sources is larger than channel coherence distance, so that the N FSO links suffer independent identically distributed (IID) fading. Meanwhile, the data bit period is far less than the channel coherence time, so the FSO transmission suffers slow, flat fading.

In this paper, we adopt OOK modulation, widely used in practical FSO systems since it is much easier to implement than higher-order modulation. The modulated input data is sent to the switch control unit, which can select one or more of the N laser sources to transmit data. The selection principle varies with different transmit-diversity schemes. In a MISO FSO system with repetition coding (RC) [17-20], all N laser sources are selected to transmit data synchronously. In Dual-TLS and Group-TLS systems, part of the N laser sources participate in sending optical signals. For TLS, SET, and SETps schemes, only one laser source is working at

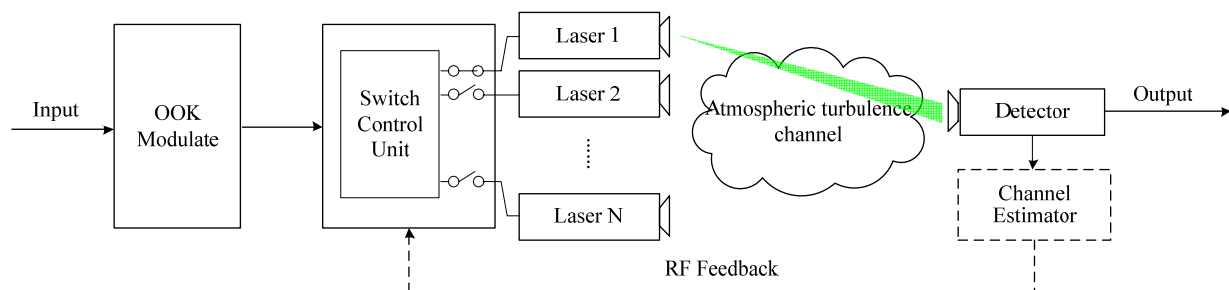


FIG. 1. FSO system model.

any moment, while the others keep silent until switching occurs.

The optical signals through a wireless optical channel, which suffers from both misalignment errors and turbulent fading, are registered by a photoelectric detector at the receiver. A channel estimator is deployed at the receiver to measure the channel-state information (CSI) and send the switching information back to the transmitter, through a low-rate radio-frequency channel. We assume that perfect CSI can be obtained, i.e. no estimation errors are considered at the estimator. Switching and selection among the N laser sources are based on this feedback information.

The photoelectric detector converts the optical power into photocurrents. Assuming that the thermal noise at the receiver may be modeled by additive white Gaussian noise (AWGN), and background illumination is removed from the electrical signal, we can express the received signal y as

$$y = \sum_{i=1}^M R h_i x + n, \quad x \in \{0, 2P_i / M\}, \quad 1 \leq M \leq N \quad (1)$$

where x is the transmitted signal, P_i is the average transmit optical power, h_i is the channel gain from the i^{th} laser source to the receiver, M is the number of current working laser sources with repetition coding, R is the detector response (assumed to be unity), and finally n is signal-independent zero-mean AWGN with variance σ_n^2 . In the assumption of a slow fading channel, the instantaneous SNR at the receiver is defined as

$$\gamma(h) = \frac{2P_t^2 h^2}{\sigma_n^2 M^2} = \bar{\gamma} \frac{h^2}{M^2} \quad (2)$$

where $\bar{\gamma} = \frac{2P_t^2}{\sigma_n^2}$ is the average SNR and $h = \sum_{i=1}^M h_i$ is the sum of M random variables. We define the average SNR as the received SNR, when there is no fading or pointing error. Note that in a transmit-diversity scheme, for the sake of fairness the sum of all working-link transmitted power should be equal to that of an SISO FSO system without a diversity scheme.

2.2. Composite Approximate Channel Model

Channel gain is susceptible to three independent factors: path loss, pointing errors, and atmospheric turbulence fading. Therefore, the channel gain of the i^{th} FSO link can be expressed as $h_i = h_i^l h_i^p h_i^a$, where h_i^l is the path loss due to geometric spread, h_i^p represents fading due to pointing errors, and h_i^a is the attenuation due to atmospheric turbulence. In the parallel transmit-diversity FSO systems described in this paper, h_i^l is deterministic and assumed to be unity hereafter. We adopt a widely used model for h_i^p , derived by Farid and Hranilovic in [3], the probability density function (PDF) of which is

$$f_{h_i^p}(h_i^p) = \frac{\varphi^2}{A_0^{\varphi^2}} (h_i^p)^{\varphi^2-1}, \quad 0 \leq h_i^p \leq A_0 \quad (3)$$

where

$$\varphi = \frac{\omega_{zeq}}{2\sigma_s}, \quad \omega_{zeq}^2 = \frac{\omega_z^2 \sqrt{\pi} \operatorname{erf}(v)}{2v \exp(-v^2)}, \quad v = \frac{\sqrt{\pi} r}{\sqrt{2}\omega_z}, \quad A_0 = \operatorname{erf}(v)^2$$

and ω_z is the beam waist at the receiver, r is the aperture radius of the detector, and σ_s^2 is the jitter variance at the receiver. We use the Gamma-Gamma turbulence model to characterize the atmospheric fading h_i^a , since it is an appropriate fading model over a wide range of turbulence conditions, and its PDF can be expressed as [24]

$$f_{h_i^a}(h_i^a) = \frac{2(\alpha\beta)^{\frac{\alpha+\beta}{2}}}{\Gamma(\alpha)\Gamma(\beta)} h_i^{\frac{\alpha+\beta}{2}-1} K_{\alpha-\beta} \left(2\sqrt{\alpha\beta h_i^a} \right) \quad (4)$$

where $\Gamma(\cdot)$ is the Gamma function, $K_{\alpha-\beta}(\cdot)$ is the $\alpha-\beta$ order modified Bessel function of the second kind, and α and β are parameters related to the small- and large-scale turbulence eddies and can be obtained as [25]

$$\alpha = \left[\exp \left(\frac{0.49\sigma_x^2}{(1+1.11\sigma_x^{12/5})^{7/6}} \right) - 1 \right]^{-1}, \quad \beta = \left[\exp \left(\frac{0.51\sigma_x^2}{(1+0.69\sigma_x^{12/5})^{5/6}} \right) - 1 \right]^{-1} \quad (5)$$

where σ_x^2 is the log irradiance variance. The PDF of channel gain h can be calculated as [24]

$$f_h(h) = \int \frac{1}{h_i^a h_i^l} f_{h_i^p} \left(\frac{h_i}{h_i^a h_i^l} \right) f_{h_i^a}(h_i^a) dh_i^a \quad (6)$$

Substituting (3) and (4) into (6), we can obtain the PDF of the i^{th} link channel gain in terms of the Meijer's G-function as [26]

$$f_{h_i}(h_i) = \frac{\alpha\beta\varphi^2}{h_i^l A_0 \Gamma(\alpha)\Gamma(\beta)} G_{1,3}^{3,0} \left[\frac{\alpha\beta}{A_0 h_i^l} h_i \mid \varphi^2 - 1, \alpha - 1, \beta - 1 \right], \quad h_i \geq 0 \quad (7)$$

However, (7) is inconvenient to compute the average BER, as the integrals and sums of Meijer's G-functions are sophisticated. Since the asymptotic behavior of the system performance is dominated by the behavior of the PDF near

the origin [2, 13], we can use the series expansion of Meijer's G-functions at zero and omit the high-order infinitesimal items in the approximation. Then the approximate channel model can be expressed as [2, 13]

$$f_{h_i}(h_i) \approx c_1 h_i^{c_2} \quad (8)$$

where c_1 and c_2 are determined by the relationship of φ^2 and β as

$$c_1 = \begin{cases} \frac{\varphi^2 (\alpha\beta)^\beta \Gamma(\alpha - \beta)}{A_0^\beta \Gamma(\alpha) \Gamma(\beta) (\varphi^2 - \beta)}, & \varphi^2 > \beta \\ \frac{\varphi^2 (\alpha\beta)^{\varphi^2} \Gamma(\alpha - \varphi^2) \Gamma(\beta - \varphi^2)}{A_0^{\varphi^2} \Gamma(\alpha) \Gamma(\beta)}, & \varphi^2 < \beta, \end{cases} \quad (9)$$

$$c_2 = \begin{cases} \beta - 1, & \varphi^2 > \beta \\ \varphi^2 - 1, & \varphi^2 < \beta \end{cases}$$

Since $h = \sum_{i=1}^M h_i$ and all links suffer IID fading, we can obtain the PDF of h using a Laplace transform. By taking the single-sided Laplace transform of the i^{th} channel gain for the PDF, we can get

$$\Phi_{H_i}(s) = c_1 \frac{\Gamma(c_2 + 1)}{s^{c_2 + 1}} \quad (10)$$

Then, using $\Phi_H(s) = \prod_{i=1}^M \Phi_{H_i}(s)$, the PDF of h can be obtained by the inverse Laplace transform of $\Phi_H(s)$ as

$$f_h(h) = \frac{[c_1 \Gamma(c_2 + 1)]^M}{\Gamma[M(c_2 + 1)]} h^{M(c_2 + 1) - 1} \quad (11)$$

For convenient calculation of average BER, we rewrite (11) in terms of SNR through the change-of-variable rule. Considering the relationship in (2), the PDF of instantaneous SNR at the receiver is given as

$$f_\gamma(\gamma) = \frac{[c_1 \Gamma(c_2 + 1)]^M}{\Gamma[M(c_2 + 1)]} \frac{M^{M(c_2 + 1)}}{2} \bar{\gamma}^{-\frac{M(c_2 + 1)}{2}} \gamma^{\frac{M(c_2 + 1)}{2} - 1} \quad (12)$$

The cumulative distribution function (CDF) corresponding to $f_\gamma(\gamma)$ is given as

$$F_\gamma(\gamma) = \frac{c_1^M}{c_2 + 1} \frac{\Gamma(c_2 + 1)^M}{\Gamma[M(c_2 + 1)]} M^{M(c_2 + 1) - 1} \left(\sqrt{\frac{\gamma}{\bar{\gamma}}} \right)^{M(c_2 + 1)} \quad (13)$$

III. ERROR RATE PERFORMANCE

In this section, the average BER expressions for SISO, RC, TLS, and MRC FSO systems are given first, since their BER performances are useful benchmarks for other transmit-diversity schemes. Then we provide the average BER expressions for SET and SETps. At last, the BER performance and system complexities of the two multiple-branch diversity schemes, namely Dual-TLS and Group-TLS, are also studied.

Following the system model described in Section II, the BER of an IM/DD with OOK modulated FSO system under the condition of instantaneous SNR is

$$P_b(e|\gamma) = Q\left(\frac{P_r h}{\sigma_n}\right) = \frac{1}{2} \operatorname{erfc}\left(\frac{\sqrt{\gamma}}{2}\right) \quad (14)$$

where $Q(\cdot)$ is the Gaussian Q-function, where $\operatorname{erfc}(\cdot)$ is the complementary error function. The average BER can be obtained by averaging the conditioned BER over the PDF of instantaneous SNR as

$$P_b(e) = \int_0^\infty f_\gamma(\gamma) P_b(e|\gamma) d\gamma \quad (15)$$

where $f_\gamma(\gamma)$ is the PDF of instantaneous SNR at the receiver.

3.1. BER of SISO, RC, and TLS FSO Systems

In a SISO or MISO FSO system, the corresponding PDF $f_\gamma(\gamma)$ is given in (12) by setting M to be 1 for SISO and N for MISO. Since all BER are calculated under IM/DD with OOK modulated FSO systems, $P_b(e|\gamma)$ is the same for different transmit-diversity schemes. Using the integral formula in [27], we have

$$\int_0^\infty \operatorname{erfc}(x) x^{a-1} dx = \frac{1}{a\sqrt{\pi}} \Gamma\left(\frac{1+a}{2}\right), \quad (16)$$

We can derive the average BER expressions for SISO and MISO with RC FSO systems as

$$P_b^{\text{SISO}}(e) = \frac{2^{c_2} c_1}{(c_2 + 1) \sqrt{\pi}} \Gamma\left(\frac{c_2 + 2}{2}\right) \bar{\gamma}^{-\frac{c_2 + 1}{2}}, \quad (17)$$

$$P_b^{\text{RC}}(e) = \frac{c_1^N}{c_2 + 1} \frac{(2N)^{N(c_2 + 1) - 1}}{\sqrt{\pi}} \frac{\Gamma\left[\frac{N(c_2 + 1) + 1}{2}\right] \Gamma(c_2 + 1)^N}{\Gamma[N(c_2 + 1)]} \bar{\gamma}^{-\frac{c_2 + 1}{2}}. \quad (18)$$

The average BER expression for the FSO system using the TLS scheme is derived as [13]

$$P_b^{TLS}(e) = \left(\frac{c_1}{c_2+1} \right)^N \frac{2^{(c_2+1)N-1}}{\sqrt{\pi}} \Gamma \left(\frac{(c_2+1)N+1}{2} \right) \bar{\gamma}^{-\frac{c_2+1}{2}N}. \quad (19)$$

Referring to the derivation of MRC receive diversity FSO systems in [21, 22], we can obtain the MRC BER expression as

$$P_b^{MRC}(e) = \left[c_1 2^{c_2} N^{(c_2+1)/2} \Gamma \left(\frac{c_2+1}{2} \right) \right]^N \frac{\bar{\gamma}^{-\frac{c_2+1}{2}N}}{N(c_2+1)\sqrt{\pi}}. \quad (20)$$

In the high SNR region, the average BER of an uncoded system under fading channels can be approximated as $P_b = (G_c \bar{\gamma})^{-G_d}$, where G_c is the coding gain, determining the shift of the average BER curves, and G_d is the diversity order, indicating how fast the BER decreases as the average SNR increases [24]. From (17), (18), (19), and (20), it can be seen clearly that the diversity orders of SISO, MISO with RC, TLS, and MISO with MRC FSO systems are respectively

$$\begin{aligned} G_d^{SISO} &= \frac{c_2+1}{2}, \quad G_d^{RC} = \frac{c_2+1}{2}N, \\ G_d^{TLS} &= \frac{c_2+1}{2}N, \quad G_d^{MRC} = \frac{c_2+1}{2}N. \end{aligned} \quad (21)$$

Note that $G_d^{RC} = NG_d^{SISO}$ and $G_d^{RC} = G_d^{TLS} = G_d^{MRC}$, which means increasing the number of laser sources can yield higher diversity orders for communication systems.

3.2. BER of SET and SETps

3.2.1 BER of SET

In the TLS scheme, the CSI of all diversity branches are simultaneously required, which increases the complexity of a practical FSO system. To overcome this disadvantage, we introduce the switch-and-examine transmit (SET) scheme. In a SET FSO system, only the CSI of the current working branch must be estimated. The switch control unit maintains the current transmission link as long as its CSI is above the predetermined threshold. When the quality of the current working branch goes bad, the control unit switches to the next laser source repeatedly, until either it finds a laser source with acceptable channel quality, or all diversity branches have been tried. If no diversity branch is above the preset threshold, the SET transmitter remains on the last laser source to communicate with the receiver.

In receive-diversity schemes, a similar scheme called switch-and-examine combining (SEC) is proposed in [28]. The switching mechanism in SET is similar to that in SEC, but the switching in SEC is achieved by the combiner at the receiver. Assuming the time for feedback and switching is

short and can be ignored, the instantaneous statistical characteristics of SNR at the output of combiner can also be used in an SET scheme. Assume that the instantaneous SNR of the current working branch is γ , and that γ_T is the pre-determined threshold SNR; the PDF of γ is derived as in [29]

$$f_{\gamma_{SET}}(\gamma) = \begin{cases} [F_{\gamma}(\gamma_T)]^{N-1} f_{\gamma}(\gamma), & \gamma < \gamma_T \\ \sum_{j=0}^{N-1} [F_{\gamma}(\gamma_T)]^j f_{\gamma}(\gamma), & \gamma \geq \gamma_T \end{cases} \quad (22)$$

where $F_{\gamma}(\gamma)$ and $f_{\gamma}(\gamma)$ are the CDF and PDF defined in (12) and (13) by setting $M=1$. The average BER of a SET FSO system is evaluated as

$$P_b^{SET}(e) = \int_0^{\infty} P_b(e|\gamma) f_{\gamma_{SET}}(\gamma) d\gamma \quad (23)$$

where $P_b(e|\gamma)$ is defined in (14). Substituting (22) into (23), we get

$$\begin{aligned} P_b^{SET}(e) &= [F_{\gamma}(\gamma_T)]^{N-1} P_b^{SISO}(e) \\ &+ \sum_{j=0}^{N-2} [F_{\gamma}(\gamma_T)]^j \int_{\gamma_T}^{\infty} P_b(e|\gamma) f_{\gamma}(\gamma) d\gamma \end{aligned} \quad (24)$$

where $P_b^{SISO}(e)$ is the average BER of a SISO FSO system derived in (17). We define the definite integral on the right of equation (24) as

$$I_1 = \int_{\gamma_T}^{\infty} P_b(e|\gamma) f_{\gamma}(\gamma) d\gamma = \frac{1}{2} \int_{\gamma_T}^{\infty} \operatorname{erfc}(\sqrt{\gamma}/2) f_{\gamma}(\gamma) d\gamma \quad (25)$$

The complementary error function $\operatorname{erfc}(x)$ in (25) can be rewritten as [30]

$$\operatorname{erfc}(x) = \frac{1}{\sqrt{\pi}} G_{1,2}^{2,0} \left[x^2 \middle| \begin{matrix} 1 \\ 0, 1/2 \end{matrix} \right] \quad (26)$$

where $G_{p,q}^{m,n} \left[z \middle| \begin{matrix} a_1, \dots, a_n, a_{n+1}, \dots, a_p \\ b_1, \dots, b_m, b_{m+1}, \dots, b_q \end{matrix} \right]$ is the Meijer's G-function.

Using the integral equation [30], we can calculate I_1 as

$$I_1 = \frac{c_1}{4\sqrt{\pi}} \left(\frac{\gamma_T}{\bar{\gamma}} \right)^{\frac{c_2+1}{2}} G_{2,3}^{3,0} \left[\frac{\gamma_T}{4} \middle| \begin{matrix} 1, \frac{1-c_2}{2} \\ -\frac{c_2+1}{2}, 0, \frac{1}{2} \end{matrix} \right] \quad (27)$$

where $\bar{\gamma}$ is the average SNR defined in (2). Finally, substituting (13), (17), and (27) into (24), after some mathe-

mathematical derivation we obtain the average BER of a SET FSO system as

$$P_b^{SET}(e) = \sum_{j=1}^N A_j \left(\frac{c_1}{c_2+1} \gamma_T^{\frac{c_2+1}{2}} \right)^j \bar{\gamma}^{-\frac{c_2+1}{2}j} \quad (28)$$

where coefficients A_j are expressed as

$$A_j = \begin{cases} \frac{c_2+1}{4\sqrt{\pi}} G_{2,3}^{3,0} \left[\frac{\gamma_T}{4} \middle| \begin{matrix} 1, (1-c_2)/2 \\ -(c_2+1)/2, 0, 1/2 \end{matrix} \right], & 1 \leq j \leq N-1 \\ \frac{2^{c_2} \Gamma[(c_2+2)/2]}{\gamma_T^{(c_2+1)/2} \sqrt{\pi}}, & j = N \end{cases} \quad (29)$$

3.2.2. BER of SETps

An SET scheme can greatly reduce system complexity compared to TLS, but this is achieved at the cost of BER performance. When no acceptable diversity link is found after all branches have been examined, SET stays at the last switching branch, which may have the worst channel quality. The switch-and-examine transmit with post-selection (SETps) scheme can compensate for this defect, i.e. the laser source with the best channel quality will be selected when none of the N diversity branches is above the preset threshold. In the case of good channel quality, the performance of SETps is close to that of SET, because few outages and switchings occur in a fine communication environment. If the channel condition goes bad, the performance of SETps will approach that of TLS, since the best branch is selected.

Following the assumptions and definitions in the derivation of average BER for SET, we can obtain the PDF of the instantaneous SNR of the current working branch as [29]

$$f_{\gamma_{SETps}}(\gamma) = \begin{cases} N [F_\gamma(\gamma)]^{N-1} f_\gamma(\gamma), & \gamma < \gamma_T \\ \sum_{j=0}^{N-1} [F_\gamma(\gamma_T)]^j f_\gamma(\gamma), & \gamma \geq \gamma_T \end{cases} \quad (30)$$

where $F_\gamma(\gamma)$ and $f_\gamma(\gamma)$ are the same as before. We evaluate the BER for SETps by averaging conditioned error probability over the instantaneous SNR of the active branch. Substituting (30) into (15), we get

$$P_b^{SETps}(e) = N \int_0^{\gamma_T} P_b(e|\gamma) [F_\gamma(\gamma)]^{N-1} f_\gamma(\gamma) d\gamma + \sum_{j=0}^{N-1} [F_\gamma(\gamma_T)]^j I_1 \quad (31)$$

where I_1 is the definite integral calculated as (27). We further define definite integral I_2 as

$$I_2 = \int_0^{\gamma_T} P_b(e|\gamma) [F_\gamma(\gamma)]^{N-1} f_\gamma(\gamma) d\gamma \quad (32)$$

Using the integral equation [30] again, we calculate I_2 as

$$I_2 = \frac{c_2+1}{4\sqrt{\pi}} G_{2,3}^{2,1} \left[\frac{\gamma_T}{4} \middle| \begin{matrix} 1-(c_2+1)N/2, 1 \\ 0, 1/2, -(c_2+1)N/2 \end{matrix} \right] \left[\frac{c_1}{c_2+1} \left(\frac{\gamma_T}{\bar{\gamma}} \right)^{(c_2+1)/2} \right]^N \quad (33)$$

Substituting I_1 and I_2 into (31), we obtain the average BER for a SETps FSO system as

$$P_b^{SETps}(e) = \sum_{j=1}^N B_j \frac{c_2+1}{4\sqrt{\pi}} \left(\frac{c_1}{c_2+1} \gamma_T^{\frac{c_2+1}{2}} \right)^j \bar{\gamma}^{-\frac{c_2+1}{2}j} \quad (34)$$

where the coefficients B_j are expressed as

$$B_j = \begin{cases} G_{2,3}^{3,0} \left[\frac{\gamma_T}{4} \middle| \begin{matrix} 1, (1-c_2)/2 \\ -(c_2+1)/2, 0, 1/2 \end{matrix} \right], & 1 \leq j \leq N-1 \\ G_{2,3}^{3,0} \left[\frac{\gamma_T}{4} \middle| \begin{matrix} 1, \frac{1-c_2}{2} \\ -\frac{c_2+1}{2}, 0, \frac{1}{2} \end{matrix} \right] + N G_{2,3}^{2,1} \left[\frac{\gamma_T}{4} \middle| \begin{matrix} 1-\frac{c_2+1}{2}N, 1 \\ 0, 1/2, -\frac{c_2+1}{2}N \end{matrix} \right], & j = N \end{cases} \quad (35)$$

3.3. BER of Dual-TLS and Group-TLS

3.3.1. BER of Dual-TLS

TLS, SET, and SETps use only one diversity branch to transmit data, which results in larger peak optical power of the working laser source than for a transmitter with several laser sources to simultaneously transmit data. However, the peak optical power should be limited, according to eye-safety standards [31]. Considering the restrictions and communication performance, we introduce the Dual-TLS FSO system, in which the transmitter selects two of the best diversity links to transmit data, and the peak power of each laser source is half that of an SISO system. Now we derive the average BER expression for Dual-TLS.

The average BER for Dual-TLS can also be evaluated by averaging the conditioned BER (14) over the PDF of the instantaneous SNR $\gamma_{Dual-TLS}$ at the receiver, and $f_{\gamma_{Dual-TLS}}(\gamma)$ is also derived from the PDF of channel gain $h = h_{N-1:N} + h_{N:N}$ at the receiver by variable substitution, where $h_{N:N}$ and $h_{N-1:N}$ are the first two best channel gains. However, $h_{N:N}$ and $h_{N-1:N}$ are no longer independent but identically distributed, so we can no longer directly derive $f_i(h)$ through a Laplace transform.

Here we abbreviate $h_{N:N}$ and $h_{N-1:N}$ respectively as h_N

and h_{N-1} , and the joint density function of h_N and h_{N-1} is given by [32]

$$f_{h_{N-1}, h_N}(h_{N-1}, h_N) = N(N-1)F_{h_i}(h_{N-1})^{N-2} f_{h_i}(h_{N-1})f_{h_i}(h_N) \quad (36)$$

where $f_{h_i}(x)$ and is the PDF of the i^{th} channel gain h_i defined in (8), and $F_{h_i}(x)$ is the CDF corresponding to $f_{h_i}(x)$. Hence, we can obtain the CDF of h as [33]

$$F_h(h) = \int_0^{h/2} \int_{h_{N-1}}^{h-h_{N-1}} f_{h_{N-1}, h_N}(h_{N-1}, h_N) dh_N dh_{N-1} \quad (37)$$

Substituting (8) and (35) into (36), we have

$$F_h(h) = \frac{c_1^N N(N-1)}{(c_2+1)^{N-2}} \int_0^{h/2} \left[h_{N-1}^{(c_2+1)(N-2)+c_2} (h-h_{N-1}) - h_{N-1}^{(c_2+1)(N-1)+c_2} \right] dh_{N-1} \quad (38)$$

Taking the derivative of $F_h(h)$, the PDF of h can be calculated as

$$f_h(h) = \frac{c_1^N N(N-1) d}{(c_2+1)^{N-2}} \frac{\int_0^{h/2} \left[h_{N-1}^{(c_2+1)(N-2)+c_2} (h-h_{N-1})^{c_2+1} - h_{N-1}^{(c_2+1)(N-1)+c_2} \right] dh_{N-1}}{dh} \quad (39)$$

After some mathematical development, $f_h(h)$ can be written as

$$f_h(h) = c_1^2 N(N-1) \left(\frac{c_1}{c_2+1} \right)^{N-2} \int_0^{h/2} \left[h_{N-1}^{(c_2+1)(N-2)+c_2} (h-h_{N-1})^{c_2} \right] dh_{N-1} \quad (40)$$

To evaluate the integral in (40), we define $t = h_{N-1}/h$, and the integration can be expressed as

$$\begin{aligned} & \int_0^{h/2} \left[h_{N-1}^{(c_2+1)(N-2)+c_2} (h-h_{N-1})^{c_2} \right] dh_{N-1} \\ &= \int_0^{1/2} \left[\left(\frac{h_{N-1}}{h} \right)^{(c_2+1)(N-2)+c_2} h^{(c_2+1)(N-2)+2c_2+1} \left(1 - \frac{h_{N-1}}{h} \right)^{c_2} \right] d \left(\frac{h_{N-1}}{h} \right) \\ &= h^{(c_2+1)N-1} \int_0^{1/2} \left[t^{(c_2+1)(N-2)+c_2} (1-t)^{c_2} \right] dt \end{aligned} \quad (41)$$

We define $W(c_2, N) = \int_0^{1/2} \left[t^{(c_2+1)(N-2)+c_2} (1-t)^{c_2} \right] dt$, which is a constant for the given parameters c_2 and N . Finally, the PDF of channel gain h at the receiver is

$$f_h(h) = \frac{N(N-1)c_1^N}{(c_2+1)^{N-2}} W(c_2, N) h^{(c_2+1)N-1} \quad (42)$$

Subsequently, the PDF of instantaneous SNR at the receiver is

$$f_{\gamma}^{\text{Dual-TLS}}(\gamma) = c_3 \left(\frac{1}{\gamma} \right)^{\frac{(c_2+1)N}{2}} \gamma^{\frac{(c_2+1)N}{2}-1} \quad (43)$$

where $c_3 = \frac{N(N-1)c_1^N 2^{(c_2+1)N-1}}{(c_2+1)^{N-2}} W(c_2, N)$. The average BER calculation for Dual-TLS is the same as for SET and SETps,

i.e. substituting (43) into (15). We finally obtain the BER expression for Dual-TLS as

$$P_b^{\text{Dual-TLS}}(e) = c_4 \bar{\gamma}^{-\frac{c_2+1}{2}N}, \quad (44)$$

where

$$c_4 = (c_2+1)(N-1) \left[\frac{c_1}{c_2+1} 2^{c_2+1} \right]^N \frac{\Gamma[(c_2+1)N]}{\Gamma[(c_2+1)N/2]} W(c_2, N).$$

From (44), we find that the diversity order of Dual-TLS is

$$G_d^{\text{Dual-TLS}} = \frac{c_2+1}{2} N \quad (45)$$

From the above analysis, we find that the diversity order of Dual-TLS is the same as that of TLS, although the number of working laser sources increases, and the CSI used for the TLS and Dual-TLS diversity schemes is the same.

3.3.2. BER of Group-TLS

There is another multiple-branch TLS transmit-diversity scheme called Group-TLS, in which all N transmitters are divided into several groups. Then the best branches from each group are selected to transmit data simultaneously. Group-TLS scheme can further reduce the peak power of each laser source. Compared to traditional MISO FSO systems, Group-TLS excludes some diversity branches with bad channel quality.

To simplify the analysis, we assume that N is even, and that all of the laser sources are grouped into $N/2$ groups, i.e., $\{h_1, h_2\}$, $\{h_3, h_4\} \cdots \{h_{N-1}, h_N\}$. According to the order statistics, the PDF of the larger channel gain in the j^{th} group is [32]

$$\begin{aligned} f_{h_{\max_j}}(h_i) &= 2F_{h_i}(h_i) f_{h_i}(h_i) \\ &= \frac{2c_1^2}{c_2+1} h_i^{2c_2+1}, 1 \leq j \leq N/2, 1 \leq i \leq N \end{aligned} \quad (46)$$

where $f(h_i)$ and $F(h_i)$ are the PDF and CDF corresponding to the channel gain of the i^{th} branch. The larger channel gains of each group are IID random variables, and the channel gain at the receiver should be

$$h^{\text{Group-TLS}} = \sum_{j=1}^{N/2} h_{\max,j} \quad (47)$$

The PDF of $h^{\text{Group-TLS}}$ can be calculated by Laplace transform. Taking the Laplace transform of (46), we have

$$\Phi_{h_{\max,j}}(s) = \frac{2c_1^2}{c_2+1} \frac{\Gamma[2(c_2+1)]}{s^{2(c_2+1)}} \quad (48)$$

Then, using the fact that $\Phi_H(s) = \prod_{j=1}^{N/2} \Phi_{h_{\max,j}}(s)$ and

taking the inverse Laplace transform of $\Phi_H(s)$, the PDF of h can be expressed as

$$f_h^{\text{Group-TLS}}(h) = \left(\frac{2c_1^2 \Gamma[2(c_2+1)]}{c_2+1} \right)^{N/2} \frac{1}{\Gamma[N(c_2+1)]} h^{N(c_2+1)-1} \quad (49)$$

By the relationship $\gamma(h) = \bar{\gamma}h^2 / M^2$ and setting $M=N/2$, we obtain the PDF of instantaneous SNR at the receiver as

$$f_\gamma^{\text{Group-TLS}}(\gamma) = \left(\frac{2c_1^2}{c_2+1} \right)^{N/2} \frac{\Gamma[2(c_2+1)]^{N/2}}{2\Gamma[N(c_2+1)]} \left(\frac{N}{2} \right)^{N(c_2+1)} \left(\frac{1}{\bar{\gamma}} \right)^{\frac{N(c_2+1)}{2}} \gamma^{\frac{N(c_2+1)}{2}-1} \quad (50)$$

Finally, through averaging the conditioned BER (14) over (50), the average BER for Group-TLS is

$$P_b^{\text{Group-TLS}}(e) = c_5 \bar{\gamma}^{\frac{c_2+1}{2}N} \quad (51)$$

$$\text{where } c_5 = \left(\frac{2c_1^2}{c_2+1} \right)^{N/2} \left(\frac{N}{2} \right)^{N(c_2+1)} \frac{1}{N(c_2+1)} \frac{\Gamma[2(c_2+1)]^{N/2}}{\Gamma[N(c_2+1)/2]}$$

From (51), we can clearly see that the diversity order of Group-TLS is

$$G_d^{\text{Group-TLS}} = \frac{c_2+1}{2}N \quad (52)$$

On the basis of the above discussion, we conclude that the diversity orders of TLS, Dual-TLS, and Group-TLS are the same, because all of these three diversity schemes use the same CSI, in other words, the channel gains of all N diversity branches.

IV. SYSTEM COMPLEXITY ANALYSIS

In this section, we discuss the complexity of TLS, SET, SETps, Dual-TLS, and Group-TLS FSO systems in the aspects of hardware structure, channel estimation rate, and lowest feedback transmission rate. We will summarize the results for each transmit-diversity scheme in Table 1.

All of these transmit-diversity FSO systems need channel estimations and feedback links, so that the transmitters can obtain CSI or switching orders. Besides, Dual-TLS and Group-TLS systems need an additional synchronization unit, for correct detection of the optical signals from different diversity branches. Therefore, Dual-TLS and Group-TLS have the most complex hardware structure.

We assume that the channel estimator at the receiver estimates K times per second, for every diversity branch. For TLS, Dual-TLS, and Group-TLS, the total number of channel estimations at the receiver is KN times per second, since the CSI of all N diversity branches are required. For SET, only the CSI of the current working branch is estimated, so the channel estimation rate is K times per second,

TABLE 1. System complexity of transmit diversity schemes

Transmit Diversity	Synchronization Unit	Channel Estimation Rate (times/second)	The Lowest Feedback Transmission Rate (bits/s)
TLS	N	KN	$K \lceil \log_2 N \rceil$
SET	N	K	P
SETps	N	$K - Q + QN$	$P - Q + Q \lceil \log_2 N \rceil$
Dual-TLS	Y	KN	$2K \lceil \log_2 N \rceil$
Group-TLS	Y	KN	$\frac{KN}{S} \log_2 S$

which is much lower than for TLS. We further assume that the channel outages occur P times per second, and that there are Q times in which the CSI of all branches are below the preset threshold, i.e. $K \geq P \geq Q$. $K - Q + QN$ channel estimations are needed at the SETps receiver, and there are P switches at its transmitter. It can be seen that the SET system needs the fewest channel estimations, followed by SETps, TLS, and Dual-TLS, while Group-TLS requires the most channel estimations.

To reduce feedback information through RF links, we compare the channel quality for each diversity branch achieved at the receiver. The feedback information is the index of the diversity branch or switching orders, instead of quantified channel gains. Therefore, for the TLS scheme, the lowest feedback transmission rate is $K \lceil \log_2 N \rceil$ bits/s, where $\lceil x \rceil$ denotes the smallest integer larger than x . Similarly, the lowest feedback transmission rate for Dual-TLS is twice that for TLS, i.e. $2K \lceil \log_2 N \rceil$ bits/s, since the indices of the two best channels must be returned. In a general Group-TLS diversity system, we assume that there are S laser sources in each group, N/S groups (assumed to be an integer), and that the index number of the best link in each group will feed back to the transmitter; then the lowest feedback transmission rate is $(KN/S) \log_2 S$ bits/s. For the special case in this paper, i.e. $S=2$, the lowest feedback transmission rate is $KN/2$ bits/s. In an SET diversity system, the lowest feedback transmission rate is P bits/s, because this system requires only one bit to be sent to the transmitter to notice an outage. Otherwise, the low-rate feedback link can keep silent, to save energy. In a SETps system, the lowest feedback transmission rate is $P-Q+Q \lceil \log_2 N \rceil$ bits/s, the additional $Q(\lceil \log_2 N \rceil - 1)$ bits/s being used to tell the transmitter to which diversity branch it should switch.

V. NUMERICAL SIMULATION AND ANALYSIS

In this section, the average BER numerical simulations of parallel transmit diversity for different FSO systems are presented. First, the asymptotic average BER performances of SET, SETps, Dual-TLS, and Group-TLS are given. The BER curves for SISO, RC, MRC, and TLS are also presented under the same channel conditions, as benchmarks for comparison. In addition, the diversity orders of SET and

SETps are also discussed. Since the approximate channel model adopted in (8) is accurate in the region of high average SNR, the asymptotic BER are calculated with average SNR above 50 dB. Second, we study how channel parameters affect the diversity orders of SET and SETps. We present the main channel parameters used during simulations in Table 2, in which the first three columns are the turbulence parameters, followed by misalignment parameters in the next three columns, and the last column contains the lesser of φ^2 and β , since the relationship between these two parameters is useful in the following analysis.

To investigate the performance of the four transmit-diversity techniques in our paper, we illustrate the BER curves of the MIMO FSO systems adopting RC at transmitters and EGC or MRC at receivers, with diversity methods in [21-23] for comparison. For the sake of fairness, we also present the BER curve of a MISO FSO system with RC and EGC as $P_b^{RC}(e)$, and a MISO FSO system with RC and MRC as $P_b^{MRC}(e)$. Furthermore, the BER curve of the TLS scheme in [13] is also given.

5.1. BER Performance of Parallel Diversity Schemes

The asymptotic average BER curves for the FSO systems using the SET scheme are given in Fig. 2. Two SET BER curves are plotted for different diversity branches, i.e. $N=3$,

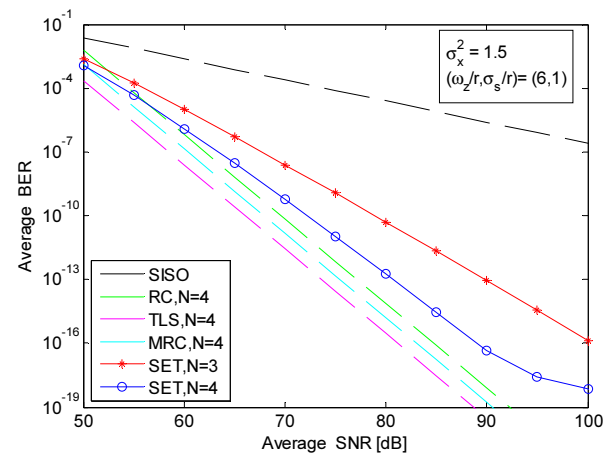


FIG. 2. Average BER for SET.

TABLE 2. Channel parameters in simulations

Case	σ_x^2	α	β	ω_z/r	σ_s/r	φ^2	$\text{Min}\{\varphi^2, \beta\}$
1	1.0	4.39	2.56	5	2	1.63	φ^2
2	1.0	4.39	2.56	5	2.5	1.04	φ^2
3	1.5	4.05	1.98	5	2	1.63	φ^2
4	1.5	4.05	1.98	6	1	9.27	β
5	1.5	4.05	1.98	6	2	2.32	β
6	4	4.34	1.31	6	1	9.27	β

4. We adopt the same channel parameters, i.e. Case 4 in Table 2. The BER with 4 diversity branches is better than that with 3 branches. Although there is only one diversity branch working in the SET scheme, more diversity branches provide better BER performance, since more branches means more useful CSI.

The BERs for SISO, RC, MRC, and TLS are also presented for comparison. It can be seen that BER performance of an FSO system using the SET diversity scheme is significantly improved, compared to that of a SISO FSO system; however, the improvement for SET is less than that for RC, MRC, or TLS. Compared to TLS, SET trades BER performance for simpler system structure and lower processing load, as discussed earlier, i.e. fewer channel estimations and lower feedback rate. As mentioned, based on (28), the diversity order of SET cannot be obtained analytically, but from Fig. 2, we find that it is between that of SISO and of TLS, i.e. $(c_2+1)/2 \leq G_d^{SET} \leq (c_2+1)N/2$. For high average SNR, we also find that the BER of SET becomes flat, which implies that G_d^{SET} decreases. When average SNR is high enough, the laser sources in SET FSO system hardly switch among diversity branches, and it can be considered a SISO FSO system in this situation. Hence, the diversity order of SET decreases in this region.

In Fig. 2, we can see that the MISO FSO system with MRC performs better than the system with RC, since the system with RC adopts the EGC scheme at the receiver. As we know that MRC is the optimal receive combining principle, therefore the BER for a MRC FSO system is better than that for an RC FSO system. Besides, both MISO FSO systems with MRC or RC perform worse than systems with TLS, because the TLS transmitter can select the best link to transmit signals, rather than no selection in an RC transmitter.

We demonstrate the asymptotic average BER for SETps in Fig. 3, and the BER performances of SISO, RC, MRC, TLS and SET are also shown for comparison. The channel parameters are the same as in Fig. 2. It can be clearly

seen that SETps performs between TLS and SET. In the first part, SETps performs almost the same as TLS, since the average SNR is not high enough, and none of the diversity branches is above the preset threshold. Since the SETps transmitter has to frequently switch among the laser sources, it works like TLS in this situation when the best link is selected. As the average SNR increases, SETps gradually tends toward SET. Because the transmit power is high enough, there is no need for the SETps transmitter to switch and select the best link often. If any of N diversity branches is above the threshold, SETps is just the same as SET. The moderate BER performance of SETps is determined by its compromise of system complexity, discussed previously. As for SET, the diversity order of SETps cannot be derived analytically. In Fig. 3, we can see that the diversity order of SETps is larger than that of SET, i.e. $G_d^{SETps} \geq G_d^{SET}$. Compared to SET, more CSI is introduced to select the best link in SETps when none branches is above the threshold.

The average BER curve for the FSO system using Dual-TLS is provided in Fig. 4. We also give the BER curves for traditional TLS, RC, and MRC with the same diversity branches, as benchmarks. In this figure we can see that the BER of Dual-TLS is slightly inferior to that of TLS, since the introduction of suboptimal branch increases ambiguity in CSI. However, Dual-TLS performs better than RC and MRC when N is greater than 2, since some diversity branches of poor quality are removed in Dual-TLS. The advantage of Dual-TLS is that it can overcome the peak power limit at the transmitter, with little BER performance loss. In (45) we derived the diversity order of Dual-TLS as $(c_2+1)N/2$, and it is the same as that of TLS and RC, which is demonstrated by the three parallel curves in Fig. 4. We also find that Dual-TLS systems with 4 branches can achieve lower BER and higher diversity order than systems with 3 branches.

We demonstrate the asymptotic average BER result for a FSO system using Group-TLS in Fig. 5. All simulation

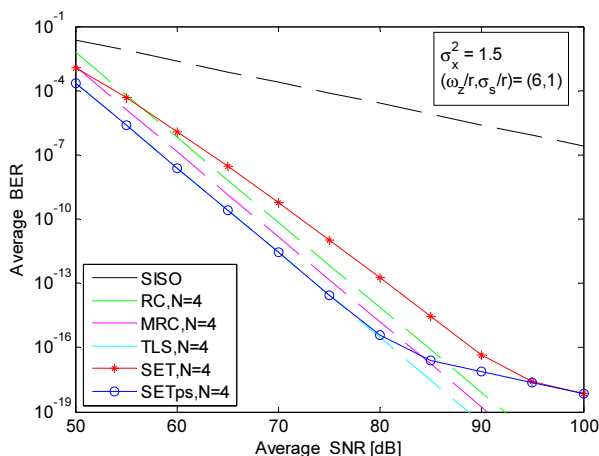


FIG. 3. Average BER for SETps.

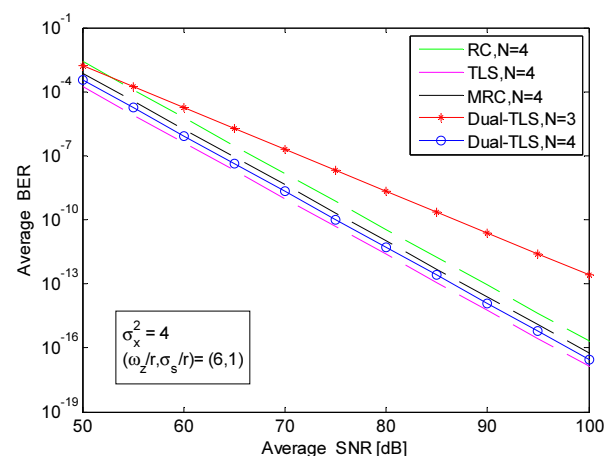


FIG. 4. Average BER curves for Dual-TLS.

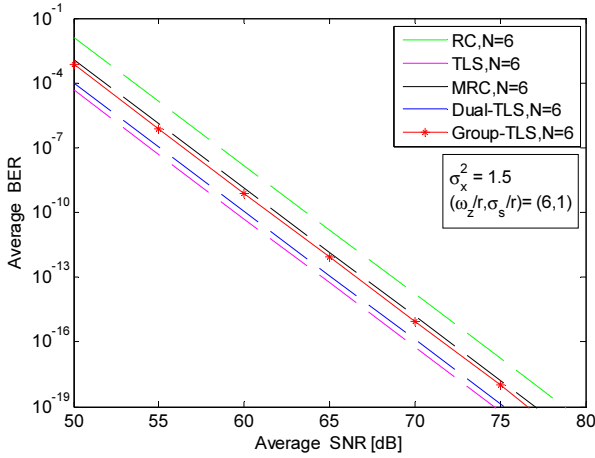


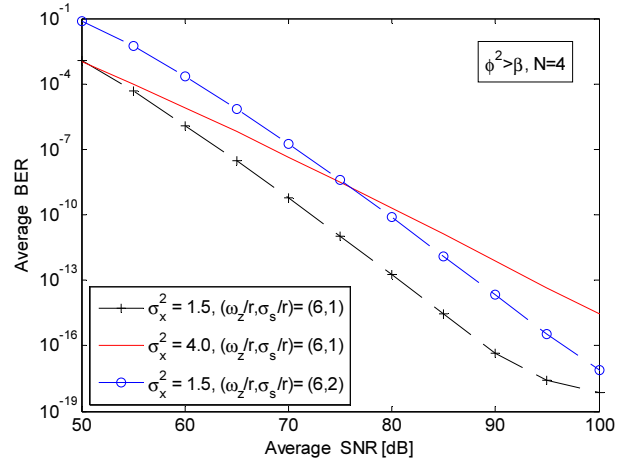
FIG. 5. Average BER curves of Group-TLS.

results are obtained under the same channel conditions and the same number of diversity branches, $N=6$. The BER curves for FSO systems with Dual-TLS, TLS, RC, and MRC are also presented, for comparison. We can see that the FSO system with Group-TLS performs much better than that with RC, and even slightly better than that with MRC, but its performance is inferior to that of Dual-TLS and traditional TLS, because introducing more branches of poor quality degrades the overall BER performance. However, Group-TLS has more working diversity branches than Dual-TLS and traditional TLS, and can further reduce peak power. Finally, similar to Dual-TLS, we can see that the diversity order of Group-TLS is the same as that of TLS and RC in Fig. 5, by the parallel curves.

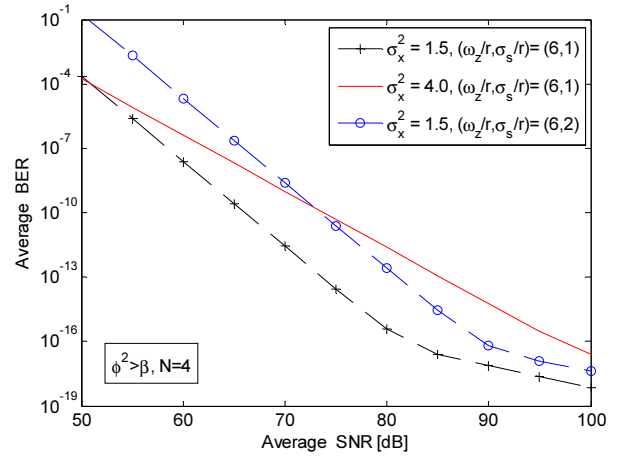
5.2. Effects of Channel Parameters on Diversity Orders of SET and SETps

A useful conclusion proposed in [13] tells us that the diversity order of TLS is determined by $\text{Min}\{\beta, \varphi^2\}$. In our study, we have derived the average BER expressions for Dual-TLS and Group-TLS, and we find that the diversity orders of Dual-TLS and Group-TLS are the same as that of TLS. In fact, the parameter c_2+1 is just $\text{Min}\{\beta, \varphi^2\}$, and the conclusion in [13] is also true for Dual-TLS and Group-TLS in this paper. However, for SET and SETps, the diversity orders still cannot be obtained analytically. Hence, in this section we examine the diversity orders of SET and SETps through numerical simulations. We give the BERs for SET and SETps under different channel conditions, and observe how the diversity orders vary.

The BERs of SET and SETps are shown in Fig. 6(a) and 6(b) respectively, when $\varphi^2 > \beta$. In the simulations we choose the channel parameters from cases 4, 5, and 6 in Table 2. In Fig. 6 we find that the two curves with the same turbulence intensity $\sigma_x^2=1.5$ are almost parallel. In addition, increasing pointing errors σ_s/r from 1 to 2 deteriorates BER performance, but it does not change the slopes of the BER curves. Note that although we increase



(a)



(b)

 FIG. 6. BER performance when $\varphi^2 > \beta$, for a system using (a) SET and (b) SETps.

the turbulence intensity, the condition $\varphi^2 > \beta$ is still satisfied; this means that the diversity orders of both SET and SETps systems are hardly affected by the pointing errors, as long as the pointing-error parameter φ^2 is larger than the atmospheric turbulence parameter β . When we fix the jitter variance $\sigma_s/r=1$ and increase the turbulence intensity σ_x^2 from 1.5 to 4.0, we find that the slopes of the BER curves change significantly. Hence, we can say that the diversity orders of SET and SETps are significantly affected by turbulence intensity when $\varphi^2 > \beta$.

Similar simulations are conducted in which the pointing-error parameter φ^2 is smaller than the turbulence parameter β , i.e. $\varphi^2 < \beta$. To satisfy this condition, we adopt the parameters corresponding to cases 1, 2, and 3 in Table 2, for which the BER curves of FSO systems using SET and SETps are given in Figs. 7(a) and 7(b) respectively. In Fig. 7 we can see that both SET and SETps have parallel BER curves when the pointing-error parameters are the same, i.e. $\left(\frac{\omega_z}{r}, \frac{\sigma_s}{r}\right) = (5,2)$. The increase of turbulence intensity from $\sigma_x^2=1.0$ to $\sigma_x^2=1.5$ does not change the slopes of the

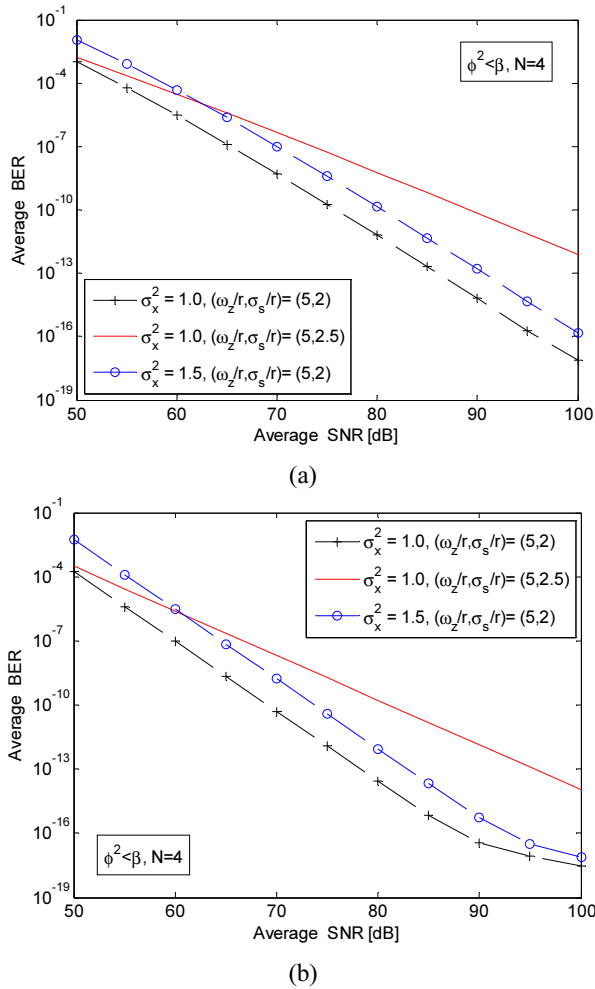


FIG. 7. BER performance when $\phi^2 < \beta$, for a system using (a) SET and (b) SETps.

BER curves. On the other hand, if we fix the turbulence intensity at $\sigma_x^2=1.0$ and change the jitter variance from $\sigma_s/r=2$ to $\sigma_s/r=2.5$, the BER curves for SET and SETps are no longer parallel. This means that the change in pointing errors has an impact on the diversity orders of both SET and SETps FSO systems. Considering the analysis in Fig. 6, we conclude that the diversity orders of SET and SETps are significantly affected by $\text{Min}\{\beta, \phi^2\}$. The conclusion for TLS in [13] is also suitable for SET and SETps in this paper.

VI. CONCLUSIONS

In this paper, we investigate the asymptotic BER performances and diversity orders of FSO links using parallel transmit-diversity schemes. The asymptotic BER expressions for FSO links with SET, SETps, Dual-TLS, and Group-TLS are derived, based on an approximate channel model. The BER performances in the region of high average SNR are presented using numerical simulations. According to

the simulations, we find that TLS performs better than SET, SETps, Dual-TLS, and Group-TLS in terms of BER. In addition, SET and SETps can reduce system complexity with performance improvement, and Dual-TLS and Group-TLS can overcome the limitation of peak power without much BER deterioration. Finally, diversity orders of the four schemes are determined by $\text{Min}\{\beta, \phi^2\}$.

REFERENCES

1. V. Dubey, D. Chadha, and V. Chandra, "Bit error rate and reliability analysis of cooperative communication in free-space optical systems," *Photon. Netw. Commun.* **28**, 92-101 (2014).
2. A. Garcia-Zambrana, C. Castillo-Vazquez, B. Castillo-Vazquez, and R. Boluda-Ruiz, "Bit detect and forward relaying for FSO links using equal gain combining over gamma-gamma atmospheric turbulence channels with pointing errors," *Opt. Express* **20**, 16394-16409 (2012).
3. A. A. Farid and S. Hranilovic, "Outage capacity optimization for free-space optical links with pointing errors," *IEEE J. Lightwave Technol.* **25**, 1702-1710 (2007).
4. M. Li and M. Cvijetic, "Coherent free space optics communications over the maritime atmosphere with use of adaptive optics for beam wavefront correction," *Appl. Opt.* **54**, 1453-1462 (2015).
5. M. Li, M. Cvijetic, Y. Takashima, and Z. Yu, "Evaluation of channel capacities of OAM-based FSO link with real-time wavefront correction by adaptive optics," *Opt. Express* **22**, 31337-31346 (2014).
6. X. M. Zhu and J. M. Kahn, "Performance bounds for coded free-space optical communications through atmospheric turbulence channels," *IEEE Trans. Commun.* **51**, 1233-1239 (2003).
7. E. Bayaki and R. Schober, "On space-time coding for free-space optical systems," *IEEE Trans. Commun.* **58**, 58-62 (2010).
8. M. Safari and M. Uysal, "Relay-assisted free-space optical communication," *IEEE Trans. Wireless Commun.* **7**, 5441-5449 (2008).
9. C. Abou-Rjeily and A. Slim, "Cooperative diversity for free-space optical communications: transceiver design and performance analysis," *IEEE Trans. Commun.* **59**, 658-663 (2011).
10. R. Boluda-Ruiz, A. Garcia-Zambrana, C. Castillo-Vazquez, and B. Castillo-Vazquez, "Adaptive selective relaying in cooperative free-space optical systems over atmospheric turbulence and misalignment fading channels," *Opt. Express* **22**, 16629-16644 (2014).
11. M. A. Khalighi and M. Uysal, "Survey on free space optical communication: A communication theory perspective," *IEEE Commun. Surveys Tuts.* **16**, 2231-2258 (2014).
12. M.-A. Khalighi, N. Schwartz, N. Aitamer, and S. Bourennane, "Fading reduction by aperture averaging and spatial diversity in optical wireless systems," *J. Opt. Commun. Netw.* **1**, 580 (2009).
13. A. Garcia-Zambrana, B. Castillo-Vazquez, and C. Castillo-Vazquez, "Asymptotic error-rate analysis of FSO links using transmit laser selection over gamma-gamma atmospheric turbulence channels with pointing errors," *Opt. Express* **20**,

- 2096-2109 (2012).
14. L. Yang, X. Q. Gao, and M. S. Alouini, "Performance analysis of free-space optical communication systems with multiuser diversity over atmospheric turbulence channels," *IEEE Photon. J.* **6**, 1-17 (2014).
 15. S. M. Navidpour, M. Uysal, and M. Kavehrad, "BER performance of free-space optical transmission with spatial diversity," *IEEE Trans. Wireless Commun.* **6**, 2813-2819 (2007).
 16. T. A. Tsiftsis, H. G. Sandalidis, G. K. Karagiannidis, and M. Uysal, "Optical wireless links with spatial diversity over strong atmospheric turbulence channels," *IEEE Trans. Wireless Commun.* **8**, 951-957 (2009).
 17. E. Bayaki, R. Schober, and R. K. Mallik, "Performance analysis of MIMO free-space optical systems in gamma-gamma fading," *IEEE Trans. Commun.* **57**, 3415-3424 (2009).
 18. S. G. Wilson, M. Brandt-Pearce, Q. L. Cao, and J. H. Leveque, "Free-space optical MIMO transmission with Q-ary PPM," *IEEE Trans. Commun.* **53**, 1402-1412 (2005).
 19. A. Garcia-Zambrana, C. Castillo-Vazquez, and B. Castillo-Vazquez, "Outage performance of MIMO FSO links over strong turbulence and misalignment fading channels," *Opt. Express* **19**, 13480-13496 (2011).
 20. N. Letzepis and A. G. I. Fabregas, "Outage probability of the Gaussian MIMO free-space optical channel with PPM," *IEEE Trans. Commun.* **57**, 3682-3690 (2009).
 21. M. R. Bhatnagar and Z. Ghassemlooy, "Performance analysis of Gamma-Gamma fading FSO MIMO links with pointing errors," *IEEE J. Lightwave Technol.* **34**, 2158-2169 (2016).
 22. K. P. Peppas and P. T. Mathiopoulos, "Free-space optical communication with spatial modulation and coherent detection over H-K atmospheric turbulence channels," *IEEE J. Lightwave Technol.* **33**, 4221-4232 (2015).
 23. J. Zhang, L. Dai, Y. Han, Y. Zhang, and Z. Wang, "On the ergodic capacity of MIMO free-space optical systems over turbulence channels," *IEEE J. Sel. Areas Commun.* **33**, 1925-1934 (2015).
 24. F. Yang, J. L. Cheng, and T. A. Tsiftsis, "Free-space optical communication with nonzero Boresight pointing errors," *IEEE Trans. Commun.* **62**, 713-725 (2014).
 25. W. P. Z. Ghassemlooy and S. Rajbhandari, *Optical Wireless Communications System and Channel Modelling with MATLAB* (CRC Press, Boca Raton, Florida, USA, 2013).
 26. H. G. Sandalidis, T. A. Tsiftsis, and G. K. Karagiannidis, "Optical wireless communications with heterodyne detection over turbulence channels with pointing errors," *IEEE J. Lightwave Technol.* **27**, 4440-4445 (2009).
 27. I. S. Gradshteyn and I. M. Ryzhik, *Table of Integrals, Series, and Products*, 7th ed. (Academic Press, San Diego, California, USA, 2007).
 28. Y. Hongchuan and M. S. Alouini, "Performance analysis of multi-branch switched diversity systems," in *Proc. Vehicular Technology Conference* (Birmingham, Alabama, USA, 2002), pp. 846-850.
 29. M.-S. A. Marvin and K. Simon, *Digital Communication over Fading Channels*, 2nd ed. (John Wiley & Sons, Inc., Hoboken, New Jersey, USA, 2005).
 30. <http://functions.wolfram.com/HypergeometricFunctions/MeijerG/>, Wolfram Research, 2015.
 31. A. A. Farid and S. Hranilovic, "Channel capacity and non-uniform signalling for free-space optical intensity channels," *IEEE J. Sel. Areas Commun.* **27**, 1553-1563 (2009).
 32. N. B. Barry, C. Arnold, and H. N. Nagaraja, *A First Course in Order Statistics* (Society for Industrial and Applied Mathematics, Philadelphia, USA, 2008).
 33. T. Eng, K. Ning, and L. B. Milstein, "Comparison of diversity combining techniques for Rayleigh-fading channels," *IEEE Trans. Commun.* **44**, 1117-1129 (1996).